Journal of Physical and Theoretical Chemistry
of Islamic Azad University of Iran, 17 (3, 4) 123-143: Fall 2020 & Winter 2021
(J. Phys. Theor. Chem. IAU Iran)
ISSN 1735-2126

Adsorption of Benzyl Paraben Dye from Aqueous Solutions Using synthesized Mn-doped PbS (PbS:Mn) nanoparticles

Elham Mousavi and Alireza Geramizadegan*

Department of Chemistry, Dashtestan Branch, Islamic Azad University, Dashtestan, Iran

Received September 2020; Accepted February 2021

ABSTRACT

Precipitation method was applied to synthesize pure and PbS (1−x) Mn (x = 0%, 5%, 10% and 15%) nanoparticles. There have been reports on the usefulness of Mn-doped PbS (PbS:Mn) nanoparticles in removal Benzyl Paraben (BP) dye from aqueous solutions. The distinctive features of this novel material were identified using different techniques like BET, XRD, SEM and FT-IR. The optimal conditions for the (BP) dye removal were found to be 2, 15 min, 100 mg/L, and 0.1 g for pH, contact time and adsorbent dosage, respectively. Regarding the Kinetic models both pseudo-first-order and pseudo-second-order diffusion models of (BP) dye revealed that the kinetic of adsorption process followed second-order equation model. After using various Isotherm models to fit the experimental equilibrium data with, the adequacy and applicability of Langmuir model has been proven. Adsorption mechanism for these adsorbents was considered to be physical which was confirmed by the E (kJ mol^{-1}) obtained from Dubinin–Radushkevich isotherm for pure PbS, PbS/Mn-5%, PbS/Mn-10% and PbS/Mn-15% were roughly -710.0, -780.0, -830.0 and -920.0 ($kJmol^{-1}$) respectively. The thermodynamic parameters including enthalpy, entropy and Gibbs energy were calculated for the adsorption of these (BP) dye using Mn-doped PbS nanoparticles suitable, spontaneous and exothermic. The maximum adsorption capacity of the (BP) dye for pure PbS, PbS/Mn-5%, PbS/Mn-10% and PbS/Mn-15% were roughly 80.0, 105.0, 131.0 and 145.0 mg/g, respectively. The findings revealed the appropriateness of Mn-doped PbS (PbS:Mn) nanoparticles as an adsorbent for (BP) dye deletion from aqueous solutions.

Keywords: Adsorption; Benzyl Paraben (BP) dye; Isotherms; Langmuir; Kinetic

1. INTRODUCTION

The severity of water pollution has been resulted from the economic development adopted by human overall the world. Textile industries consume huge quantities of water and generate an enormous amount of impurities including dyes, detergents, additives, suspended solids, aldehydes, heavy metals, non-biodegradable matter, and insoluble substances [1]. According to recent reports, more than one million dyes are commercially available with annual production of over 7×10^5 tons. The textile

*Corresponding author: geramialireza42@gmail.com, elmosavi325@gmail.com

industry worldwide consumes approximately1×10^4 tons of dyes annually and discharges nearly 100 tons/year of dyes into wastewater [2]. Wastewaters of industries like textile, paper, rubber, plastic, leather, cosmetic, food, and drug industries contain dyes and pigments which are hazardous and can cause allergic dermatitis, skin irritation, cancer and mutation in living organisms [3]. Synthetic dyes have severe effects on environment as well as living beings. Many dyes are toxic and carcinogenic in nature [4]. Along with these harmful properties most dyes are inert and non-biodegradable [5]. The importance of the potential pollution of dyes and their intermediates has been incited with the toxic nature of many dyes, different mutagenic effects, skin diseases and skin irritation and allergies. Moreover, they are dangerous because their microbial degradation compounds, such as benzidine or other aromatic compounds have carcinogenic effect [6].

Parabens as a series of p-hydroxybenzoate acids are synthetic chemicals utilized as preservatives and antimicrobial in various products, especially personal care products (PCPs), pharmaceuticals, food, beverages, and industrial [4,5]. The four widely used preservatives in daily-use products include Butylparaben (BP), ethylparaben (EP), methylparaben (MP), and propylparaben (PP),) which are either used singly or in combination [6]. However, studies have previously indicated that continued exposure to parabens even in low concentrations can cause alteration of the endocrine system pathway of vertebrates. Recently, evidence of parabens have been identified in human breast tumor tissues have been presented and were also found to as cause of male infertility as a result of testis mitochondrial dysfunctions [7,8].

In comparison with other conventional techniques (ion exchange, biological treatments, and electrolysis), adsorption is one of the most successful and uncomplicated techniques for deletion of toxic and noxious contaminations. Its popularity is due to advantages including higher efficiency lower waste, and facile and mild operational conditions. The successfulness of adsorption techniques in deletion of pollutants especially those which are extremely stable in biological degradation process via economically accomplishable mild ways [9-11]. Thus, the extensive utilization of adsorption techniques for deletion of numerous chemicals from aqueous solutions seems logical [12,13]. For deletion of dyes pollutants, nanomaterial's based adsorbents are highly proposed [14,15]. Physical and chemical properties of the adsorbent are determinative in efficient applicability of an adsorption process. Among the essential properties of an adsorbent, high adsorption capacity, recoverability and availability at economical cost are mentionable. Nowadays, diverse potential adsorbents have been used for deletion of specified organics from water samples. From this perspective, an extensive survey was conducted on magnetic nanoparticles (MNPs) as novel adsorbents with high adsorption capacity, large surface area, and small diffusion resistance. As an instance, for dissociation of chemical species like environmental pollutants, metals, dyes, and gases, magnetic nanoparticles were used [16,17].

Lead Sulphide (PbS) refers to a semiconducting material of an IV–VI group with a narrow band gap [18]. PbS nano crystals, in the past, have thoroughly been scrutinized due to the strong quantum confinement of both electrons and holes [19]. Synthesis of PbS nano powders is possible via a diverse range of physical and chemical methods [20]. To be more specific, doped PbS with various metal

ions due to its controllable physical behavior have received special attention [21]. Paramagnetic behavior of PbS doping of magnetic atoms Mn has been studied. Also, considering artificial materials especially metamaterials is worth noticing [22].

In this article, with the help of precipitation method, Pure Mn-doped PbS (PbS:Mn) nanoparticles were synthesized. Then, characterization of synthesized nanopowders were done using X-ray diffraction (XRD), scanning electron microscopy (SEM), Fourier transform infrared (FT-IR) spectra and reflectance spectrum in the wavelength range of 200-1200 nm. Cubic structure and single phase nature of pure and Mn-doped PbS have been revealed in X-ray diffraction studies. For the deletion of (BP) dye from aqueous solutions this adsorbent was employed. Accordingly for the deletion of (BP) dye from wastewater we had a good reason to provide and utilize Pure Mn-doped PbS (PbS:Mn) nanoparticles as inexpensive, safe and environmentally friendly adsorbents. Therefore, experimental conditions (pH of solution, contact time, initial dyes concentration and the dyes removal percentage as response) were scrutinized and optimized. To fit the experimental equilibrium data, different isotherm models of Langmuir, Freundlich, and Dubinin–Radushkevich were applied. The applicability and usefulness of the Langmuir model was proven by the obtained outcomes. Kinetic models of pseudo-first-order, pseudo-second-order diffusion along with elovichmodels demonstrated that the kinetic of adsorption process was controlled by the pseudo-second-order model. The effectiveness of Pure Mn-doped PbS (PbS:Mn) nanoparticles in deleting (BP) dye from wastewater was confirmed.

2. EXPERIMENTAL

2.1. Reagents and instruments

UV–vis spectrophotometer (jasco, Model UV–vis V-530, Japan). Fourier transform infrared (FT-IR) spectra were recorded on a PerkinElmer (FT-IR spectrum BX, Germany). The morphology of samples was studied by scanning electron microscopy (SEM: KYKY-EM 3200, Hitachi Company, China) under an acceleration voltage of 26kV). The pH/Ion meter (model-728, Metrohm Company, Switzerland, Swiss) was used for the pH measurements. Laboratory glassware was kept overnight in 10% nitric acid solution.

2.2. Preparation of Stock Solution

Benzyl Paraben (BP) dye, sodium hydroxide, hydrochloric acid, Iron Oxide. They were supplied from Merck (Darmstadt, Germany). For the pH adjustment, Universal buffer solutions were prepared from 1 ml of acetic acid / boric acid / phosphoric acid (1.0 M). All used chemicals were of reagent grade and utilized without further purification.

2.3. Preparation of Mn-doped PbS (PbS:Mn) nanoparticles

The synthesis of pure and Mn-doped PbS (PbS:Mn) nanoparticles was executed at ambient temperature by the precipitation method. In this process for preparing pure PbS first 0.01 mol of $Pb(NO_3)_2$ was dissolved in 25 ml of dw (deionized water) for 15 min under consecutive stirring. The XRD patterns of $PbS(1-x)$ Mnx nanoparticles (x = 0%, 5%, 10% and 15%). The nanoparticle PbS was synthesized in reactive solution prepared using lead nitrate $[Pb(NO_3)_2]$ and thiourea $[SC(NH_2)_2]$ with concentration of 0.06 M and 0.25 M. The NaOH pellets were used as a base medium and its concentration was set to 0.6 M. 150 mL of all the above solutions were prepared separately, using distilled water as a solvent and mixed together in a beaker. 0.1 M of EDTA was

added into the solution as a complexing agent, which can easily bind the metal ions. The reactive vessel with solution was immersed into oil bath maintained at 80^{oC}.

$$Pb(NO_3)_2 + 2NaOH \rightarrow Pb(OH)_2 + 2NaNO_3$$

$$Pb(OH)_2 + 2NaNO_3 \rightarrow Na_4Pb(OH)_6$$

$$Na_4Pb(OH)_6 \rightarrow 4Na^+ + HPbO_2^- + 3OH^- + H_2O$$

In the alkaline medium, the thiourea decomposes and releases S_2 ions. Pb_2S ions precipitate from the solution leading to the formation of PbS [27].

$$SC(NH_2)_2 + OH^- \rightarrow CH_2N_2 + H_2O + SH^-$$

$$HPbO_2^- + SH^- \rightarrow PbS + H_2O + SH^-$$

Three samples of Mn-doped PbS nanoparticles was provided likewise through implementing change in the concentration of $Mn(OAc)_2$ $4H_2O$ 15mol %. Typically Mn-doped PbS nanoparticles were synthetized by dissolving specific amount of $Mn(OAc)_2{\cdot}4H_2O$ in 25 ml DW(deionized water). The stirring continued vigorously for 15 min. Continous washing of the obtained mixture and oven drying of it led to the synthesis of Mn-doped PbS nanoparticles [23].

2.4. Sorption of (BP) dye ontoMn-doped PbS (PbS:Mn) nanoparticles

For binary adsorption of (BP) dye, a batch process applying Mn-doped PbS (PbS:Mn) nanoparticles was employed while all experiments were implemented in a barrel-shaped glass ware by adding 0.1g of sorbent to 100 ml of PH 2.0 for (BP) dye as perfect value. At ambient temperature, the barrel-shaped vessel was submerged in bath for 15 min and the centrifugation of the solutions was done subsequently. Then with the help of UV–Vis spectrophotometer set at wavelengths 670 nm for (BP) dye, non-adsorbed dye contents were ascertained.

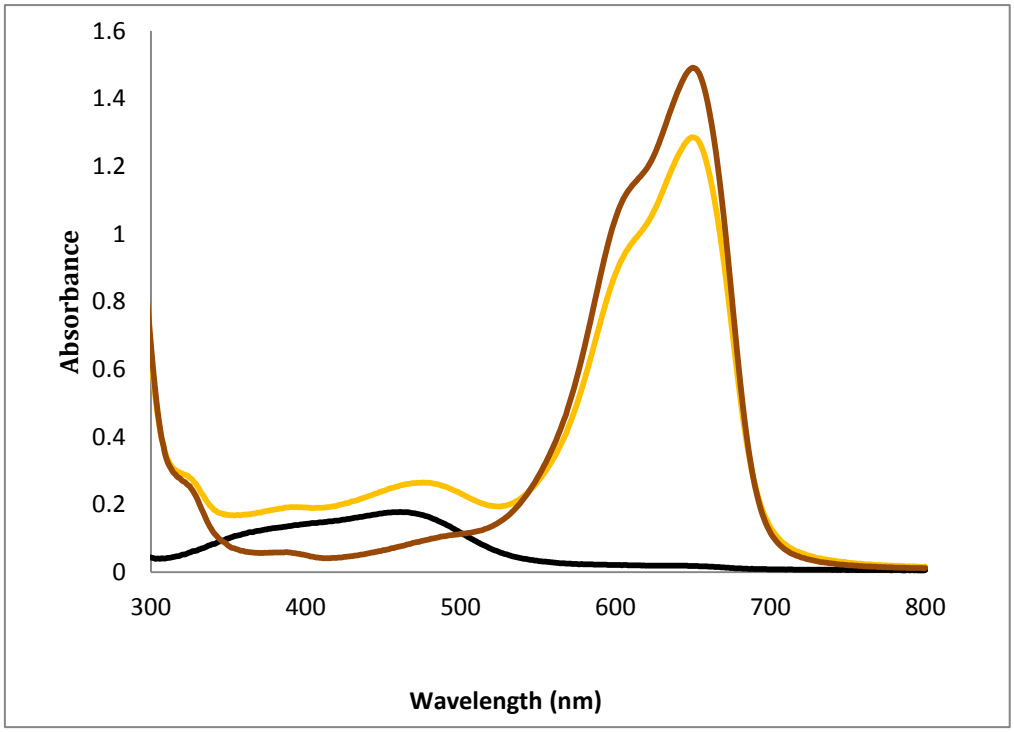

Fig. 1. Sorption spectra adsorbent of pure PbS, PbS/Mn-10% and PbS/Mn-15%nanoparticles.

2.4. Batch adsorption (BP) dye adsorption process

To ascertain the (BP) dye adsorption isotherm onto Pure Mn-doped PbS (PbS:Mn) nanoparticles and also to determine its kinetic properties, batch adsorption tests were executed. First, 500 mL solution containing 100 mg/L concentration of (BP) dye was provided. When adjustment of initial pH of the solution was done by 0.01N HCl / 0.01N NaOH aqueous solution, no further adjustments were performed during the trials. By dividing this 500 mL solution into ten samples of 50 mL, ten flasks (100 mL) containing fixed adsorbent dose of 100 mg/L were provided. With a help of an orbital shaker, these flasks were agitated at a steady rate of 200 rpm and a controlled temperature of 25^{oC}. At fixed time intervals, one flask was withdrawn from orbital shaker (1 at 18 min) and analyzed for remaining dyes in the sorbate solution. The measurment of (BP) dye concentration in the solution was carried out applying double beam UV–visible spectra. The calculation of the equilibrium adsorbed dyes quantities (q_e (mg/g)) was done employing the ensuing equation:

$$\%\, Removal = \frac{(C_0 - C_t)}{C_0} \times 100 \qquad (1)$$

C_0 and C_t refer to the initial concentration of dyes (mg/L) and the concentration of dye at any time (mg/L), respectively.

$$q_e = \frac{(C_0 - C_e)V}{W} \qquad (2)$$

In the above equation, q_e, C_0, C_c, V and W refer to adsorption capacity (mg/g), the primary concentrations of dyes (mg/mL), the equilibrium concentrations of dyes (mg/mL), the volume of the aqueous phase (ml), and the weight of the adsorbent (g), respectively.

3. RESULTS AND DISCUSSION

3.1. Characterization and evaluation of Pure Mn-doped PbS (PbS: Mn) nanoparticles as an adsorbent.

3.1.1. BET analysis of Mn-doped PbS (PbS:Mn) nanoparticles

bulk density, surface area, and loss of mass on ignition are shown in Table 1. The bulk density affects the rate of adsorption of BP dye solution by Mn-doped PbS (PbS:Mn) nanoparticles. In the present study, the bulk density was less than 1.0 indicating that the materials are in fine nature and hence enhanced the adsorption of BP dye from aqueous solution [25]. The moisture content (0.5%) was determined, even though it does not affect the adsorption power, dilutes the adsorbents, and therefore necessitates the use of additional weight of adsorbents to provide the required weight. The surface area of Mn-doped PbS (PbS:Mn) nanoparticles in the present research study was 250 m^2/g and is higher than a low cost agro-based adsorbent such as Mn-doped PbS (PbS:Mn) nanoparticles (45.231 m^2/g and 1.34×10^{-2} cm^3/g).

3.1.2. FTIR analysis

In Fig. 3: FTIR spectra for pure and Mn-doped PbS nanoparticles (x = 15%) are exhibited. By FTIR analysis almost detecting the vibrational frequencies for stretching bonds in PbS molecule is impossible which is a good indication for this fact that PbS doesn't display any definite absorption signals in the range 400-4000cm^{-1}. Because of the presence of the hydroxyl group in the compound, the existed vibration modes at 3437 cm^{-1} is assignable to the O–H broad absorption mode. attributed to the C-H tensile vibration 2935 cm^{-1} of the methylene group acetate in $Mn(OAc)_2{\cdot}4H_2O$ for synthesis of Mn-doped PbS nanoparticles. The wide absorption near 1300-1000cm^{-1} is a good indication of the presence of the C–O bond. The O–H bending vibration from the

water molecules adsorbed into the surface resulted in the absorption band at 1645 cm^{-1}. In addition indefinite points might prove that no significant difference existed between the FTIR spectra of pure and Mn-doped PbS nanoparticles [25].

Table 1. Characteristics of the Mn-doped PbS (PbS:Mn) nanoparticles

Parameter	pH	Moisture (%)	Bulk density (gmL^{-1})	Surface area (m^2/g)	Particle size rangr (μm)	Loss of mass on ignition
Value	7.0	0.5	0.45	250	45-250	0.6235

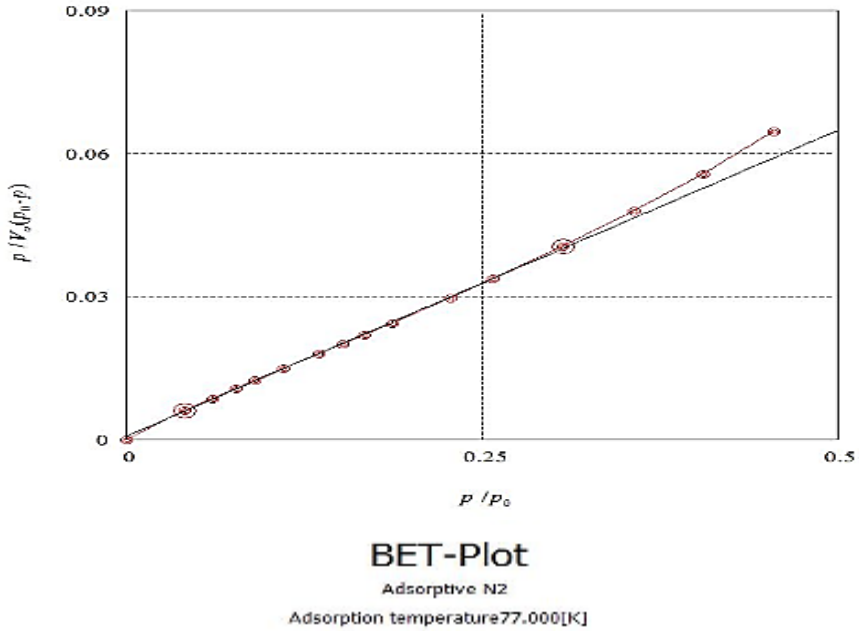

Fig. 2: N_2 adsorption–desorption isotherms of pure and 15 mol% Mn-doped PbS nanoparticles.

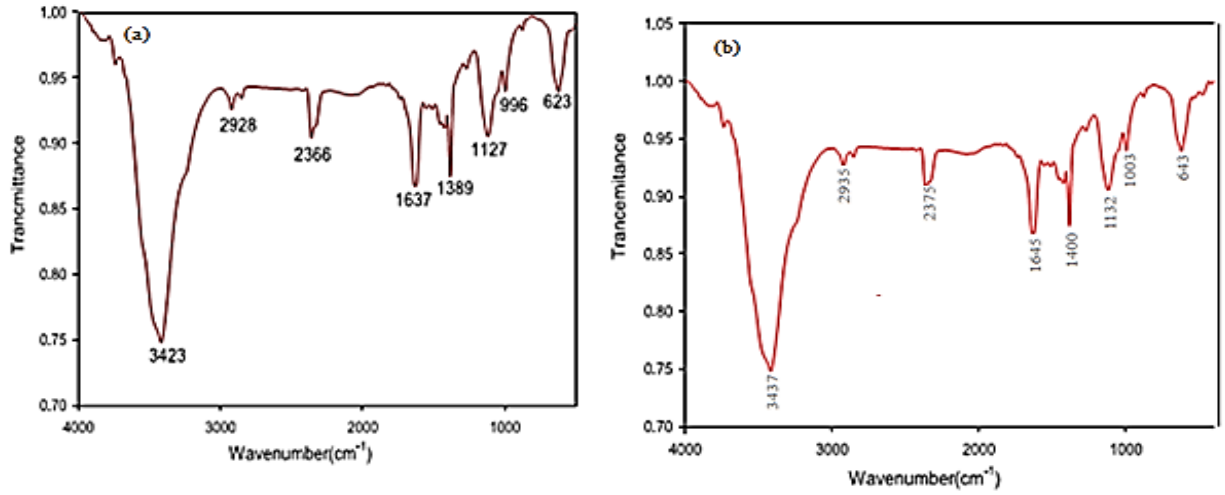

Fig. 3. (a) FTIR spectra of Mn-doped PbS nanoparticles before BP dye and (b) FTIR spectra of Mn-doped PbS nanoparticles after BP dye.

3.1.3. XRD analysis

Different x-ray emission peaks are Mn-doped PbS nanoparticles, the adsorption of BP dye and based in (fig.4), show peaks at 2θ= 25.8, 30.5, 42.8, 51.2 53.7, 62.4, 68.3, 71.5 and 79.2° belong to the lattice planes of (111), (200), (220), (311), (222), (400), (331), (420) and (422) planes pertain to the pure cubic phase of PbS [26]. Obviously the perfect crystalline nature of the material was proven after functionalizing with Mn-doped PbS nanoparticles however the great intensity of signal at 25.8 (111) and 30.5 (200) confirmed that there has been a slight amount of material in amorphous state. The perfect synthesis of Mn-doped PbS nanoparticles is obvious through looking at XRD pattern of crystal.

3.1.4. Surface morphology

With the help of SEM micrograph, the morphological properties and particle size distribution of the PbS (1−x) Mn x nanoparticles (x=15%) were obtained and shown in Fig. 5. It has been detected that the particles shape were globose and their sizes varied since they agglomerate. Knowledge of the particle sizes led us to estimate the average particle size in the range of 37-44 nm which were close to those estimated in XRD analysis [27].

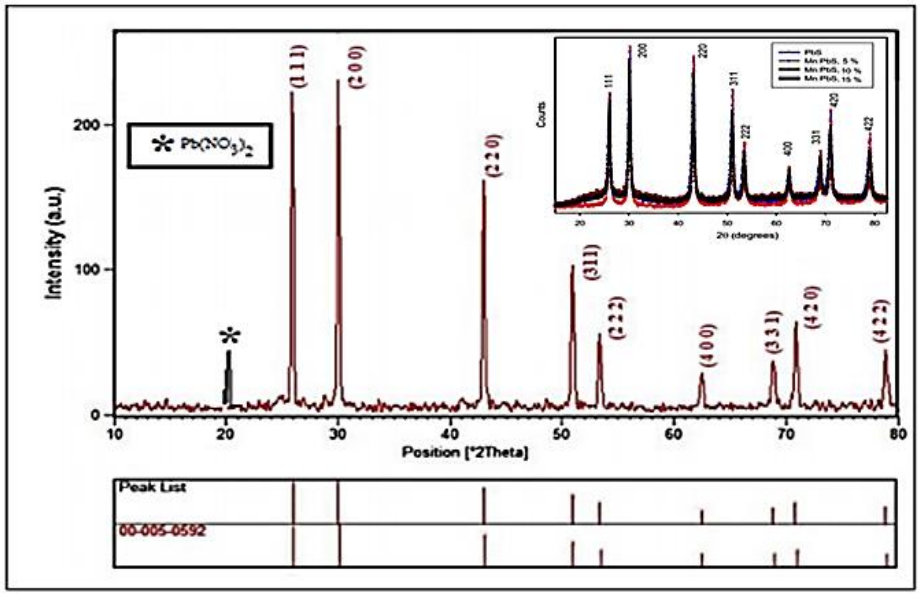

Fig. 4. The XRD patterns of PbS (1-x) Mnx nanoparticles (x = 0%, 5%, 10% and 15%).

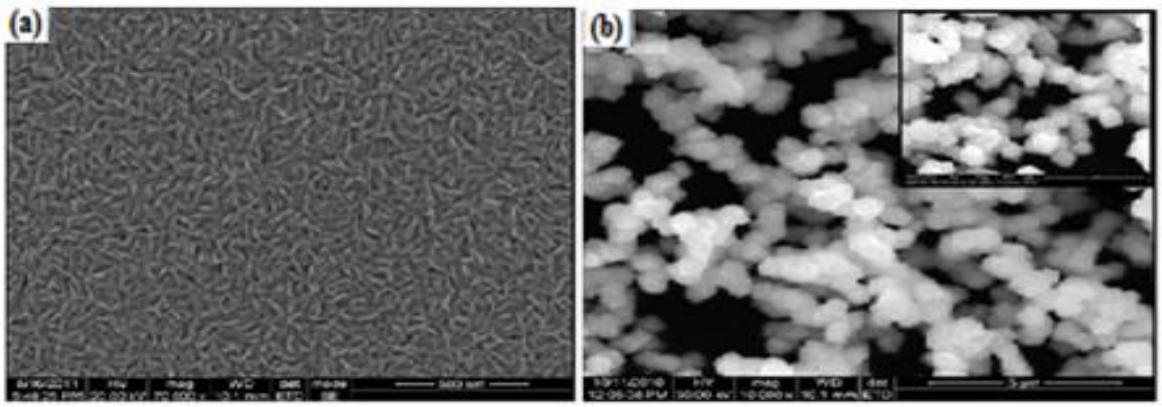

Fig. 5. The (a) SEM image pure PbS nanoparticles and (b) SEM image Mn-doped PbS nanoparticles**.**

3.2. Impact of buffer on the adsorption of (BP) dye

In this section, the best type of buffer and its volume for maximum absorption BP dye with Mn-doped PbS nanoparticles are investigated. To this step, the procedure is as follows: In 50 ml balloons, separately 1 ml of BP dye (100 mg L^{-1}) and a volume of each type of acetic acid / boric acid / phosphoric acid buffer and then 1 ml of 1 ml with Mn-doped PbS nanoparticles (0.1g), pH= 2, to the solution inside the balloon and after (15 min), the adsorption reaction of the solutions by the device read a spectrophotometry and UV–Visible spectrum. The results are shown in (Fig. 6). Based on the results, 1 ml of acetic acid buffer shows the highest percentage for the determination of BP dye, so acetic acid / tri chloro acetate buffer (3.0 M) to adjust the pH solution as the optimal buffer.

3.3. Impact of pH on the adsorption

The impact of pH value in the adsorption process is considerable. The deletion of (BP) dye as a function of pH by varied sorbent is shown in (Fig. 7). To control optimum pH for the highest deletion of (BP) dye, the measurment of equilibrium adsorption of (BP) dye was done at varied pH levels from 2.0 to 9.0 through adjusting the initial (BP) dye concentrations at 100 ppm and the summary of the obtained outcomes are displayed [28]. The highest deletion percentages of (BP) dye was procured at pH = 2.0. This amount for pure purePbS was 78.3, for PbS/Mn-5% was 80.9, for PbS/Mn-10% was 84.2 and for PbS/Mn-15% was 87.4%. Abatement in (BP) dye deletion at pH <2 happened due to competition of (BP) dye with H^+. Additionally in highly acidic pH, sharp concentration of H^+ set the scene for protonation of nitrogen atoms on the surface of adsorbents and provoked the reduction of interaction with (BP) dye and surface of adsorbents. Both reasons of precipitation of hydroxide and conversion of (BP) dye provoked the reduction in (BP) dye deletion at pH >2. This phenomenon obstructed the access of (BP) dye molecules to adsorption sites and culminated in less adsorption of (BP) dye [29].

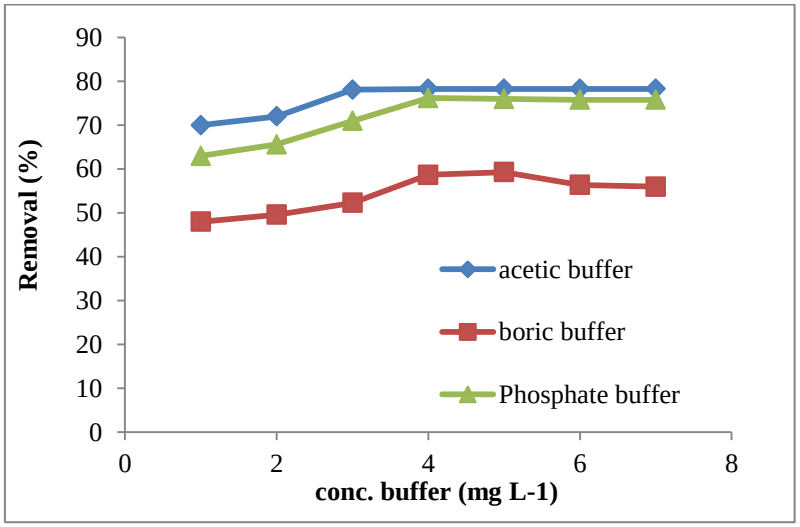

Fig. 6. The efficacy Buffer concentration of (BP) dye deletion [(BP) dye conc = 100 mg L^{-1}; pH=2.0; contact dose adsorbent = 0.1 g; stirring speed= 180 rpm; temp= 25^{o}C].

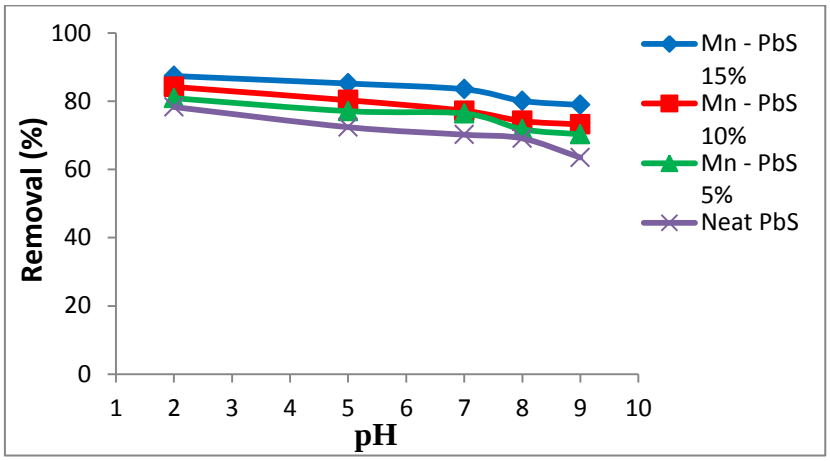

Fig. 7. Impact of pH on (BP) dye deletion [(BP) dye conc = 100 mgL^{-1}; adsorbent dose = 0.1 g L^{-1}; contact time = 15 min; stirring speed = 180 rpm; temp = 25°C].

3.4. Impact of the contact time on the adsorption of (BP) dye

The net result of contact time on sorption of (BP) dye using synthesized PbS, PbS/Mn-5%, PbS/Mn-10% and PbS/Mn-15%nanoparticles is exhibited in (Fig. 8). A little change in sorption rate was observed at 16 min for pure PbS nanoparticles, at 14 min for PbS/Mn-5% and PbS/Mn-10%, and at 12 min for PbS/Mn-15%. The sorption rate leveled off little by little until when no considerable increasing was observed in the (BP) dye adsorption and the deletion finally reached equilibrium [30]. Thus, at contact times of 16, 14, 14 and 12 min, the maximum of removal percentages were 88.4%, 83.6%, 79.0% and 73.5% for pure PbS, PbS/Mn-5%, PbS/Mn-10% and PbS/Mn-15% nanoparticles respectively.

3.5. Impact of Temperature

The net result of temperature on the adsorption of (BP) dye is shown in (Fig. 9). Based on the obtained results, a gradual boost in the removal percentage for pure PbS/Mn-15% nanoparticles from 68.8% to 87.0%, for pure PbS/Mn-10%nanoparticles from 63.0% to 81.4%, for pure PbS/Mn-5% nanoparticles from 60.0% to 80.0% and for pure PbS nanoparticles from 59.0% to 76.0% was observed. Also, the endothermic nature of the adsorption became apparent considering the above results. The probability of diffusion of adsorbate due to the porosity of adsorbent cannot be disregarded and since the process is endothermic therefore, any boost in the temperature will help the adsorbate transport with in the pores of adsorbent [31].

3.6. Absorption isotherms

The fraction of sorbate molecules which are partitioned between liquid and solid phases at equilibrium is descibed by adsorption isotherm. With the help of four adsorption isotherms of Langmuir, Freundlich, Temkin, and Dubinin-Radushkevich isotherms, adsorption of (BP) dye onto pure PbS, PbS/Mn-5%, PbS/Mn-10% and PbS/Mn-15% nanoparticles was modeled [32]. A detailed delineation of adsorption equilibrium isotherm rests on mathematical relation of the quantity of adsorbed target per gram of adsorbent (q_e(mg/g)) to the equilibrium non-adsorbed quantity of dyes in solution (C_e (mg/L) at determined temperature [33,34]. To scrutinize the adsorption

isotherm of adsorption, three models of Langmuir adsorption isotherm, Freundlich adsorption isotherm and Dubinin–Radushkevich (D-R) isotherms were employed.

1) Based on Langmuir adsorption isotherm model: no interaction existed amongst adsorbed molecules and adsorption process on homogeneous surfaces. The ensuing equation presents Langmuir model [35]:

$$C_e/q_e = 1/K_L q_{max} + C_e/q_{max} \quad (3)$$

In the above equation C_e (mg/L) refers to the equilibrium concentration, q_e (mg/g) shows the adsorption capacity in the aqueous solution and q_{max} (mg/g) signify the maximum adsorption capacity of the adsorbents in the aqueous solution. K_L as a constant is relative to binding energy of the sorption system (L/mg) (Fig. 10 a).

2) Based on Freundlich adsorption isotherm model, the multilayer adsorption of an adsorbate onto a heterogeneous surface of an adsorbent can be described. The linear formula of Freundlich isotherm model is shown below:

$$\text{Log } q_e = \log k_f + 1/n \log Ce \quad (4)$$

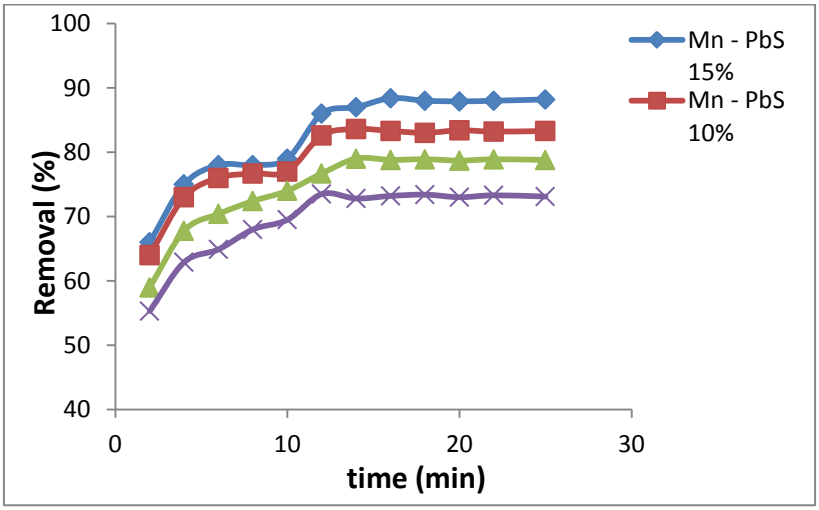

Fig. 8.net result of time on (BP) dye deletion [(BP) dye conc = 100 mg L^{-1}; pH=2.0; contact dose adsorbent = 0.1 g; stirring speed= 180 rpm; temp= 25°C].

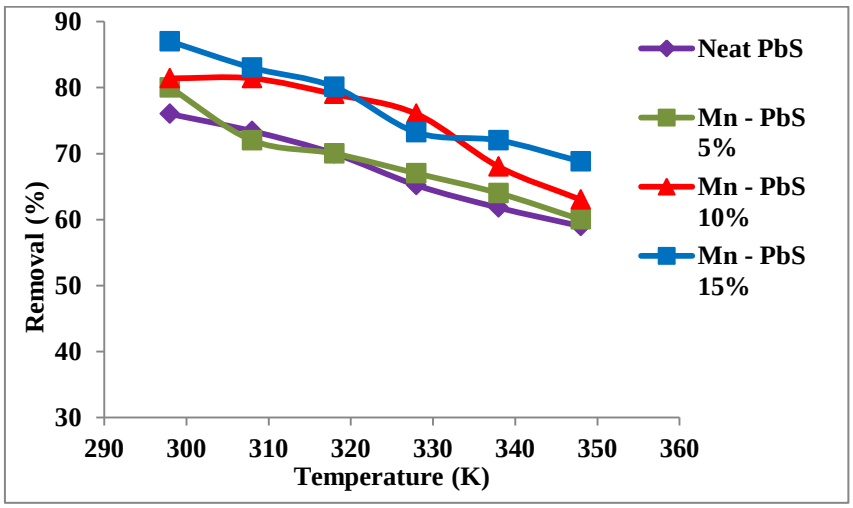

Fig. 9. net result of temperature on (BP) dye deletion [(BP) dye conc = 100 mg L^{-1}; adsorbent dose = 0.1g L^{-1}; pH = 2.0; contact time = 15 min, stirring speed = 180 rpm].

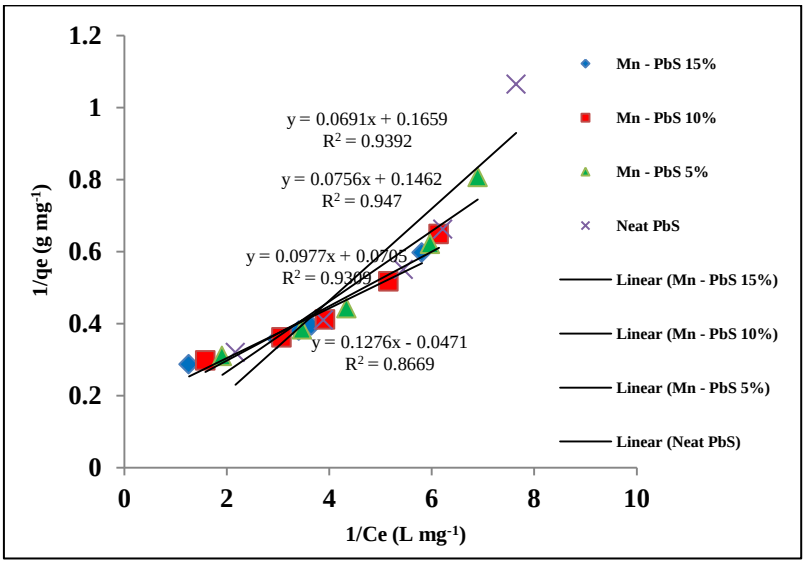

Fig. 10. (a) Langmuir isotherm for the Adsorption of (BP) dye onto Synthesized Pure Sorbent PbS, PbS/Mn-5%, PbS/Mn-10% and PbS/Mn-15%nanoparticles. [(BP) dye conc = 100 mg L^{-1}; adsorbent dose = 0.1g L^{-1}; pH = 2.0; contact time = 15 min, stirring speed = 180 rpm; temp= 25^{o}C].

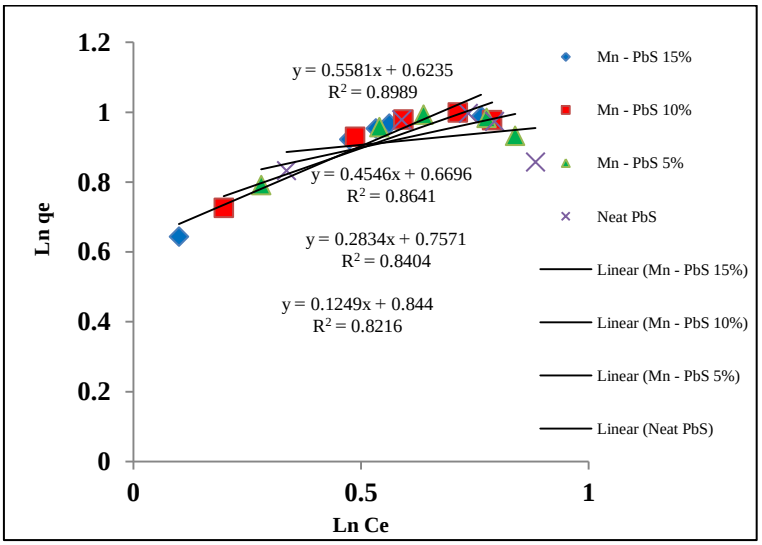

Fig. 10. (b) Freundlich isotherm for the Adsorption of (BP) dye onto Synthesized Pure Sorbent PbS, PbS/Mn-5%, PbS/Mn-10% and PbS/Mn-15%nanoparticles. [(BP) dye conc = 100 mg L^{-1}; adsorbent dose = 0.1g L^{-1}; pH = 2.0; contact time = 15 min, stirring speed = 180 rpm; temp= 25^{o}C].

The Freundlich isotherm constants are the K_f (the adsorption capacity) and n (intensity of a given adsorbent) (Fig. 10 b).

As shown in Fig. 10 b and c, in both models the values of the constants are procured from the slope and the position. The results of the fit and the constants of both models for (BP) dye are presented in Table 2. The values of **n** for pure PbS, PbS/Mn-5%, PbS/Mn-10% and PbS/Mn-15% nanoparticles were 8.064, 3.534, 2.203 and 1.792, respectively. The values between 1 and 10 for n in the adsorption process are favorable [36]. All the correlation coefficients and parameters acquired for the isotherm models from Table 2 showed that the Langmuir isotherm is the perfect model to show the

adsorption of (BP) dye for pure PbS, PbS/Mn-5%, PbS/Mn-10% and PbS/Mn-15% nanoparticles adsorbent.

3) Based on Dubinin–Radushkevich (D-R) isotherms model the nature of adsorption is investigated. The following formula presents the linear form of this model:

$$Lnq_e = lnq_m - \beta\varepsilon^2 \quad (5)$$

β in the above equation refers to the activity coefficient relatative to mean sorption energy (mol^2 / kJ^2), and ε stands for the Polanyi potential that can be procured from the ensuing equation:

$$\varepsilon = RTln(1+1/Ce) \quad (6)$$

R stands for the ideal gas constant (8.3145 J/mol K) and T for the absolute temperature (K) (Fig. 10 c). E_a refers to the free energy change of adsorption (kJ/mol) that stands in need of transferring 1 mol of ions from solution to the adsorbent surface and can be procured from the ensuing equation [37]:

$$E_a = 1/(-2\beta)^{1/2} \quad (7)$$

E_a< 8 kJ/mol in this model is a good indication that the mechanism of adsorption is Physical while 8 >E_a< 20 kJ/mol is a good indication of chemical ion exchange and E_a> 20 kJ/mol well indicate that the mechanism of (BP) dye adsorption is chemical [38]. The E value of -700.0 is for pure PbS, -770.1 for PbS/Mn-5%,-817.12 for PbS/Mn-10% and -903.0 for PbS/Mn-15% nanoparticles. Therefore, it is suggested that (BP) dye adsorption for pure PbS, PbS:Mn-5%, PbS/Mn-10% and PbS/Mn-15% nanoparticles adsorbent is physical.

3.7. The adsorption kinetic investigations

Different parameters relative to both the state of the solid (mainly with very heterogeneous reactive surface) and to physico- chemical conditions under which the adsorption tookplace are considered effective in the adsorption of a solute by a solid in aqueous solution [39]. Four kinetic model of 1- pseudo-first-order,2-pseudo-second-order and 3-Elovich model were applied to the data to scrutinize the adsorption kinetics of dye [40,41]. The adsorption kinetic data was described by the Lagergren pseudo-first order model [42]. The following clearly express the Lagergren:

$$\frac{dq_t}{dt} = k_1(q_e - q_t) \quad (8)$$

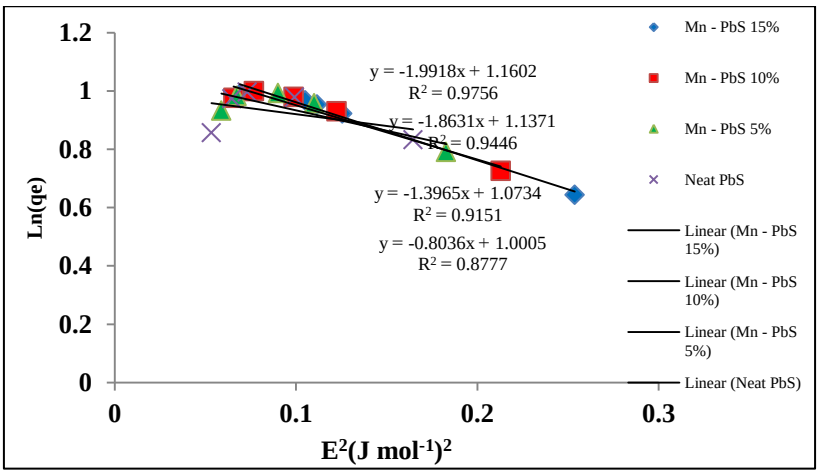

Fig. 10. (c) Dubinin-Radushkevich isotherm for the Adsorption of (BP) dye onto Synthesized Pure Sorbent PbS, PbS/Mn-5%, PbS/Mn-10% and PbS/Mn-15%nanoparticles. [(BP) dye conc = 100 mg L^{-1}; adsorbent dose = 0.1g L^{-1}; pH = 2.0; contact time = 15 min, stirring speed = 180 rpm; temp= 25°C].

Table 2. varied isotherm constants and correlation coefficients computed for the Adsorption of (BP) dye onto Synthesized Pure Sorbent PbS, PbS/Mn-5%, PbS/Mn-10% and PbS/Mn-15%nanoparticles. [(BP) dye conc = 100 mg L^{-1}; adsorbent dose = 0.1g L^{-1}; pH = 2.0; contact time = 15 min, stirring speed = 180 rpm; temp= 25°C]

Isotherm	parameters	Value of parameters For PbS/Mn-15%	Value of parameters For PbS/Mn-10%	Value of parameters For PbS/Mn-5%	Value of parameters For pure PbS
Langmuir	Q_m (mg g^{-1})	144.93	133.33	103.09	78.74
	K_L (L mg^{-1})	0.418	0.514	1.386	2.702
	R^2	0.939	0.947	0.930	0.866
Freundlich	n	1.792	2.203	3.534	8.064
	K_F $(mg)^{1-n}$ $L^n g^{-1}$	4.198	4.667	5.715	6.982
	R^2	0.8989	0.8641	0.8152	0.7216
Dubinin-Radushkevich (DR)	Q_m (mg g^{-1})	120.2	100.8	60.5	41.8
	E (kj mol^{-1})	-903.0	-817.12	-770.1	-700.0
	R^2	0.8756	0.8446	0.725	0.816

1) The ensuing shows the pseudo-first-order model in an equation:

$$\ln(q_e - q_t) = \ln q_e - K_1 t \quad (9)$$

That K_1 shows the rate constant of adsorption (min^{-1}) qe and qt refer to the quantities of (BP) dye adsorbed per unit mass of the adsorbent (mgg^{-1}) at equilibrium and time t, respectively. The followings present the way of their calculation:

$$q_e = (C_i - C_e)\, V/m \quad (10)$$

$$q_t = (C_i - C_t)\, V/m \quad (11)$$

C_t (mg L^{-1}) in the above equation stands for the (BP) dye concentrations at time t.

2) The ensuing equation clearly expresses the pseudo-second-order model:

$$\frac{t}{q_t} = \frac{1}{k_{ad} q_e^2} + \frac{1}{q_e} t \quad (12)$$

That kad presents the rate constant of equation (g mg^{-1} min^{-1}) which can be calculated from the plots of t/q_t versus t. and $h = k_{ad} q_e^2$ (mg g^{-1} min^{-1}) fig. 11.

3) Elovich equation is expressed as:

$$q_t = \frac{\ln(hB)}{B} + \frac{\ln(t)}{B} \quad (13)$$

Where β shows the desorption constant (mg g^{-1} min^{-1})

3.7. Adsorption thermodynamics

For the adsorption processes, 3 thermodynamic parameters of 1-Gibbs free energy change (ΔG°), 2- enthalpy change (ΔH°) and 3- entropy change ΔS° were considered. Their computation becomes possible through utilizing the ensuing equations [43]:

$$\Delta G^\circ = -RT \ln K_{ad} \quad (14)$$

$$\ln K_{ad} \frac{\Delta H^\circ}{RT} + \frac{\Delta S^\circ}{R} \quad (15)$$

From a plot of lnKe against 1/T, a graph (Fig.12) is provided. By considering the slope of this graph ΔG can be acquired. In Table.4, the summary of the thermodynamic parameter outcomes for the adsorption of (BP) dye onto Synthesized Pure Sorbent PbS and PbS/Mn-15%nanoparticles at diverse temperatures is demonstrated.

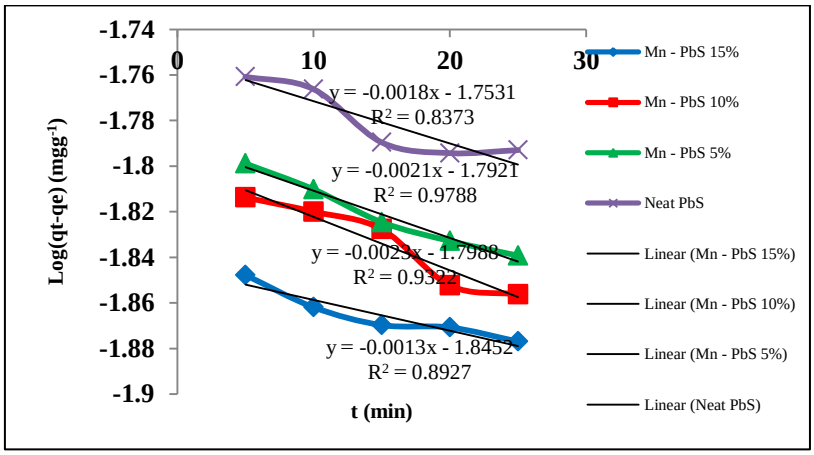

Fig. 11. (a) Pseudo-first order model for Adsorption of (BP) dye onto Synthesized Pure Sorbent PbS, PbS/Mn-5%, PbS/Mn-10% and PbS/Mn-15%nanoparticles. [(BP) dye conc = 100 mg L^{-1}; adsorbent dose = 0.1g L^{-1}; pH = 2.0; contact time = 15 min, stirring speed = 180 rpm; temp= 25°C].

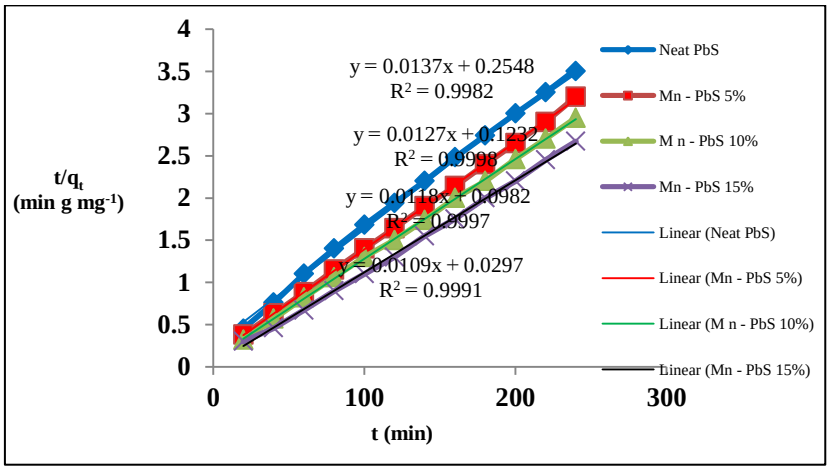

Fig. 11. (b) Pseudo-second order model for Adsorption of (BP) dye onto Synthesized Pure Sorbent PbS, PbS/Mn-5%, PbS/Mn-10% and PbS/Mn-15%nanoparticles. [(BP) dye conc = 100 mg L^{-1}; adsorbent dose = 0.1g L^{-1}; pH = 2.0; contact time = 15 min, stirring speed = 180 rpm; temp= 25°C].

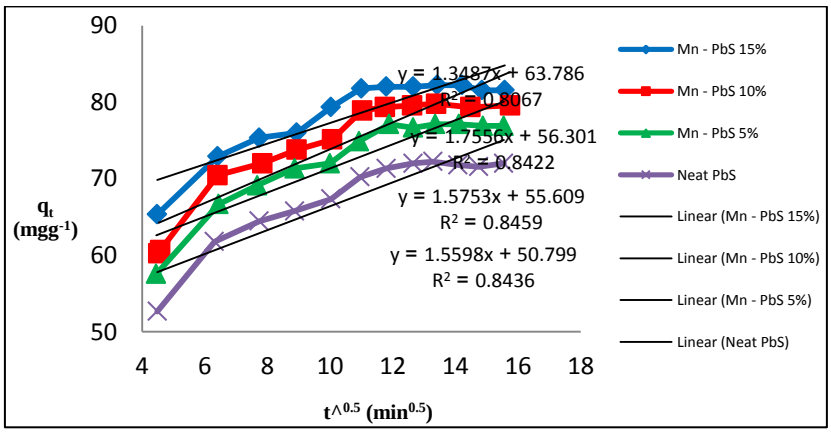

Fig. 11. (c) Elovich model for Adsorption of (BP) dye onto Synthesized Pure Sorbent PbS, PbS/Mn-5%, PbS/Mn-10% and PbS/Mn-15%nanoparticles. [(BP) dye conc = 100 mg L^{-1}; adsorbent dose = 0.1g L^{-1}; pH = 2.0; contact time = 15 min, stirring speed = 180 rpm; temp= 25°C].

Table 3: juxtaposition of the Kinetic parameters for Adsorption of (BP) dye onto Synthesized Pure Sorbent PbS, PbS/Mn-5%, PbS/Mn-10% and PbS/Mn-15%nanoparticles. [(BP) dye conc = 100 mg L^{-1}; adsorbent dose = 0.1g L^{-1}; pH = 2.0; contact time = 15 min, stirring speed = 180 rpm; temp= 25°C].

Model	parameters	Value of parameters For PbS/Mn-15%	Value of parameters For PbS/Mn-10%	Value of parameters For PbS/Mn-5%	Value of parameters For PbS
pseudo-First-order kinetic $\log(q_e - q_t) = \log(q_e) - (\frac{k_1}{2.303})t$	$q_{e,cal}$ (mg/g)	17.7	17.5	15.7	16.9
	K_1 (min^{-1})	0.034	0.038	0.036	0.03
	R^2	0.8967	0.9322	0.9788	0.8373
pseudo-Second-order kinetic $t_{/q_t} = \frac{1}{k_2 q_e 2} + \left(\frac{1}{q_e}\right) t$	$q_{e,cal}$ (mg/g)	55.01	48.10	39.26	30.18
	K_2(g/mg min)	0.082	0.057	0.062	0.051
	R^2	0.9999	0.9997	0.9998	0.9982
Elovich $q_t = \frac{1}{\beta} ln(\alpha\beta) + \frac{1}{\beta}\ln(t)$	β (mg/g min)	0.0281	0.0263	0.0288	0.0414
	α (g/mg)	54.334	54.233	62.998	75.137
	R^2	0.8436	0.8459	0.8422	0.8067

The estimation of ΔG^o values became possible via employing the equation adsorption of (BP) dye. As can be seen in (Fig.12), with any increase in the temperature from 298.0 to 348.0 K, a steep reduction in the Synthesized Pure Sorbent PbS and PbS/Mn-15%nanoparticles adsorbent was observed which confirms the exothermicity nature of the process. The values of the thermodynamic parameters (Table 4) [44] were computed using the plots. The feasiability and spontaneity nature of the process was revealed by the negative value of ΔG^o. On the other hand, the exothermicity nature of adsorption was proven by the negative value of ΔH^o and the value of ΔS^o was a good indication of change in the randomness at the derived Synthesized Pure Sorbent PbS and PbS/Mn-15% nanoparticles solution interface during the sorption. The fact that ΔG^o values up to -4.7 J/mol (BP) dye are accordant with electrostatic interaction between sorption sites and the (BP) dye (physical adsorption) has been reported. The obtained ΔG^o values in this article for (BP) dye are <-5 J/mol suggesting the predominancy of the physical adsorption mechanism in the sorption process.

3.8. Recycling of the Adsorbent

The ability of recovering and reusing of the adsorbent was tested in several steps of adsorption and desorption. The result is shown in (Fig. 13). As shown in Figure 95/0 of (BP) dye was desorbed from the adsorbent after first cycle and after 6 cycles, there were slight changes in (BP) dye onto Synthesized Pure Sorbent PbS, PbS/Mn-5%, PbS/Mn-10% and PbS/Mn-15%nanoparticles desorption. So, it was concluded that the desired removal of 88.2% can be achieved after 6 cycles.

3.9. Comparison for the amount of dyes removed with other adsorbents

Table.5, demonstrates the max adsorption capacities of varied adsorbents for the deletion of dyes comparatively. The type and density of active sites in adsorbents which are responsible for adsorption of

metal ions from the solution result in the variation in (q_{max}) values. The outcomes of the table clearly show that the sorption capacity of utilized sorbent in the current study is significantly high. In general, morphology, particle size and distribution, and surface structure of this sorbent were effective in its successful outcomes.

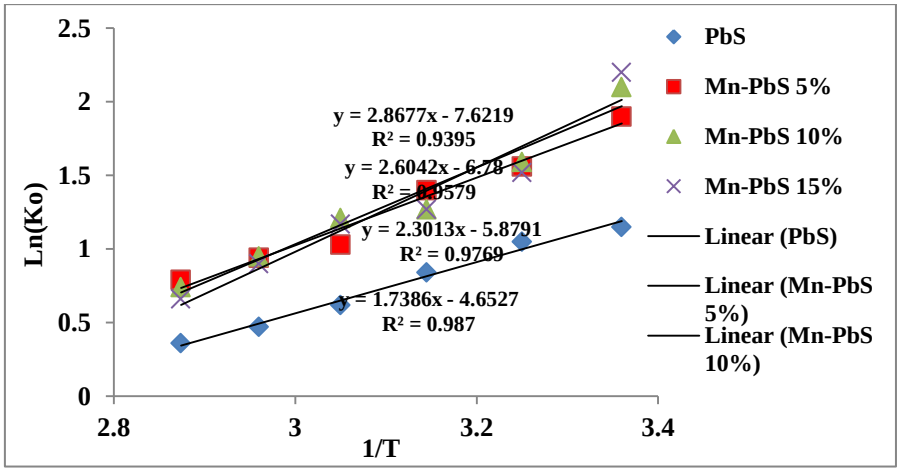

Fig. 12. Plot of ln Kc vs. 1/T for the estimation of thermodynamic parameters for the adsorption of (BP) dye onto Synthesized Pure Sorbent PbS and PbS/Mn-15%nanoparticles [(BP) dye conc = 100 mg L^{-1}; adsorbent dose = 0.1g L^{-1}; pH = 2.0; contact time = 15 min, stirring speed = 180 rpm; temp= 25^{o}C].

Table 4. The thermodynamic parameters for the adsorption of (BP) dye onto Synthesized Pure Sorbent PbS and PbS/Mn-15%nanoparticles. [(BP) dye conc = 100 mg L^{-1}; adsorbent dose = 0.1g L^{-1}; pH = 2.0; contact time = 15 min, stirring speed = 180 rpm; temp= 25^{o}C]

(BP) dye (100mg/L)	T (K)	Kc	value of ΔS^{o} (kJ/mol. K)	value of ΔH^{o}(kJ/mol)	value of ΔG^{o}(kJ/mol)
Sorbent PbS	298	8.62	-63.4	-23.84	-5.337
	308	4.56			-3.885
	318	3.57			-3.365
	328	3.2			-3.172
	338	2.39			-2.448
	348	1.98			-1.976
Sorbent PbS/Mn-5%nanoparticles	298	8.09	-56.4	-21.65	-5.18
	308	4.88			-4.06
	318	3.55			-3.35
	328	3.27			-3.24
	338	2.57			-2.653
	348	2.13			-2.188
Sorbent PbS/Mn-10%nanoparticles	298	4.38	-40.95	-16.12	-3.66
	308	4.38			-3.78
	318	3.76			-3.5
	328	3.17			-3.15
	338	2.13			-2.12
	348	1.7			-1.54
Sorbent PbS/Mn-15%nanoparticles	298	3.17	-38.683	- 14.455	-2.858
	308	2.76			-2.6
	318	2.33			-2.236
	328	1.87			-1.706
	338	1.62			-1.356
	348	1.43			-1.035

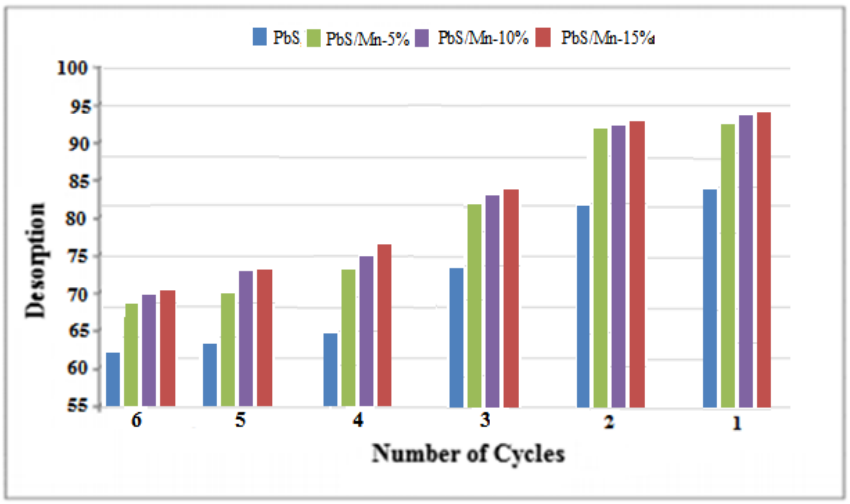

Fig. 12. Desorption of (BP) dye onto Synthesized Pure Sorbent PbS, PbS/Mn-5%, PbS/Mn-10% and PbS/Mn-15%nanoparticles. [(BP) dye conc = 100 mg L^{-1}; adsorbent dose = 0.1g L^{-1}; pH = 2.0; contact time = 15 min, stirring speed = 180 rpm; temp= 25^{o}C].

Table 5. Juxtaposition of the adsorption capacities of different adsorbents for the adsorption of dyes onto nano sorbent removal by batch method

Dyes	Adsorbent	Dosage sorbent (g)	Adsorption capacity (mg g^{-1})	References
Methyl Paraben and Propyl Paraben	MWTACC	0.1	85.9 and 90.0	[5]
Propyl Paraben	TiO_2NPs-AC	0.025	120.0	[6]
Methyl Paraben	Activated carbon (AC)	0.1	7.52	[7]
Propyl Paraben	Il-MNP-ßCD-TDI	0.1	18.48	[8]
Methyl Paraben and Propyl Paraben	ß-cyclodextrin (ß-CD) toluene-2,6-diisocyanate.	0.4	0.1019 and 0.2551	[10]
purpurin dye	Mn-doped $Fe2O_4$ NPs-AC	0.027	60.0	[14]
Naphthpl Yellow S dye	Sorbent Waktu kontak	0.2	143.72	[17]
Benzyl Paraben dye	Mn-doped PbS (PbS:Mn) NPs	0.1	145.0	Present study

4. CONCLUSION

The selection of Mn-doped PbS (PbS:Mn) nanoparticles as an effecacious adsorbent for the deletion of (BP) dye from aqueous solutions has been investigated. In the present study, the applicability of Mn-doped PbS (PbS:Mn) nanoparticles as an available, useful, and affordable for deleting (BP) dye from aqueous solutions has been confirmed. The desired values of the pH, adsorbent dosage, (BP) dye concentration, and contact time were chosen to be 2, 0.1g, 100 mg/L, and 12, 14, 14 and 16 min for pure PbS, PbS/Mn-5%, PbS/Mn-10% and PbS/Mn-15% nanoparticles respectively. The influence of different process parameters demonstrated that the percentage of adsorption lessened with boost in initial (BP) dye concentration while it rose with boost in adsorbent dose. At pH 2.0, the highest (BP) dye deletion by adsorbent was observed. To fit the experimental equilibrium data, different isotherm models were employed. The suitability and applicability of Langmuir model was proven by the obtained results. The highest

removal percentages of (BP) dye was obtained at pH = 2.0 which was 78.3 for pure PbS, 80.9 for PbS/Mn-5%, 84.2 for PbS/Mn-10% and 87.4% for PbS/Mn-15%. Also the highest adsorption capacities (q_{max}) were found to be about 80.0 mg/g for pure PbS, 105.0 mg/g for PbS/Mn-5%, 131.0 mg/g for PbS/Mn-10% and 145.0 mg/g for PbS/Mn-15%. Adsorption mechanism for these adsorbents was considered to be physical which was confirmed by the E (kJ mol^{-1}) obtained from Dubinin–Radushkevich isotherm for pure PbS, PbS/Mn-5%, PbS/Mn-10% and PbS/Mn-15% were roughly -710.0, -780.0, -830.0 and -920.0 (kJ mol^{-1}) respectively. The kinetics scrutiny decided that (BP) dye deletion followed pseudo second-order rate equation. Thermodynamic parameters of free energy (ΔG^0), enthalpy (ΔH^0) and entropy (ΔS^0) of adsorption were determined using isotherms. ΔH^0= -23.9 kJ/mol, ΔG^0= -5.337 kJ/mol and ΔS^0= -63.3 kJ/mol.K and ΔH^0= -14.5 kJ/mol, ΔG^0= -2.858 kJ/mol for PbS and ΔS^0= -38.9 kJ/mol.K for PbS/Mn-15%. The fact that the sorption process was endothermic was well reflected by the negative value of (ΔG^o, ΔH^o and ΔS^o) which on its own expressed the affinity of Pure Mn-doped PbS (PbS:Mn) nanoparticles synthesis for deleting (BP) dye. In addition the possibility of recycling the adsorbent was well proved by desorption studies. Based on the results from the linear regression-based analysis, it was revealed that the derived empirical models represented a passable prediction of performance for pure PbS, PbS/Mn-5%, PbS/Mn-10% and PbS/Mn-15% nanoparticles with significant determination coefficients (R^2= 0.994-0.984). Additionally, the statistical outcomes guaranteed that the recommended equations could favourably be employed for the adsorption of (BP) dye from aqueous solutions. Further investigations on the suitability of this adsorbent for the deletion of other materials have been suggested. Also it was suggested to investigate on the suitability of this adsorbent in industrial application. The findings proved the appropriateness of the present precedure for the successful deletion of Pollutants from aqueous solution.

ACKNOWLEDGEMENTS

The authors gratefully acknowledge partial support of this work by the Islamic Azad University, Branch of Dashtestan Iran.

REFERENCES

[1] M. Zubair, I. Ihsanullah, N. Jarrah, A. Khalid, M.S. Manzar, T.S. Kazeem, M.A. Al- Harthi, Starch-NiFe-layered double hydroxide composites: efficient removal of methyl orange from aqueous phase.J. Molecular Liquids. 249 (2018) 254–264.

[2] I. Anastopoulos, I. Pashalidis, A.G. Orfanos, I.D. Manariotis, T. Tatarchuk, L. Sellaoui, A. Bonilla-Petriciolet, A. Mittal, A. Nunez-Delgado, Removal of caffeine, nicotine and amoxicillin from (waste) waters by various adsorbents. A review. J. Environ. Management. 261 (2020) 110236.

[3] C. Arora, S. Soni, S. Sahu, J. Mittal, P. Kumar, P.K. Bajpai, Iron based metal organic framework for efficient removal of methylene blue dye from industrial waste. J. Molecular Liquids. 284 (2019) 373-352.

[4] V. Kumar, P. Saharan, A.K. Sharma, A. Umar, I. Kaushal, Y. Al-Hadeethi, B. Rashad, A. Mittal, Silver doped manganese oxide-carbon nanotube nanocomposite for enhanced dye-sequestration: Isotherm studies and RSM modelling approach. J. Ceramics International. 46 (2020) 10309–10319.

[5] G. P. Mashile, A. Mpupa, A. Nqombolo, K. M. Dimpe, Philiswa, N. Nomngongo, Recyclable magnetic waste tyre activated carbon-chitosan composite as an effective adsorbent rapid and simultaneous removal of methylparaben and propylparaben from aqueous solution and wastewater. J. Water. Process. Eng. 33 (2020) 101011.

[6] M. Pargari, F. Marahel, B. Mombini Godajdar, Ultrasonic Assisted Adsorption of Propyl Paraben on Uultrasonically Synthesized TiO_2 nano particles loaded on activated carbon: Optimization, kinetic and equilibrium studies. J. Desal. Water. Treat. 112 (2020) 1-9.

[7] P. Atheba, N. Guadi, B. Allou, P. Drogui, A. Trokourey, Adsorption kinetics and thermodynamics study of butylparaben on activated carbon coconut based. J. Encapsul. Adsorpt. Sci. 8 (2018) 39–57.

[8] M. Yusoff, N. Yahaya, N. Saleh, M. Raoov, A study on the removal of propyl, butyl, and benzyl parabens via newly synthesised ionic liquid loaded magnetically confined polymeric mesoporous adsorbent. RSC Adv. 8 (2018) 25617–25635.

[9] A. Asfaram, M. Ghaedi, F. Yousefi, M. Dastkhoon, Experimental design and modeling of ultrasound assisted simultaneous adsorption of cationic dyes onto ZnS: Mn-NPs-AC from binary mixture, Ultrason Sonochem. 33 (2016) 77-89.

[10] Y. P. Chin, S. Mohamad, M. R. Bin Abas, Removal of parabens from aqueous solution using ß-cyclodextrin cross-linked polymer. Int. J. Mol. Sci. 11 (2010) 3459–3471.

[11] S. Bagheri, H. Aghaei, M. Ghaedi, M. Monajjemi, K. Zare, Novel Au–Fe_3O_4 NPs Loaded on Activated Carbon as a Green and High Efficient Adsorbent for Removal of Dyes from Aqueous Solutions Application of Ultrasound Wave and Optimization, Eur. J. Anal. Chem. 13(3) (2018) 1-10.

[12] S. Ito, S. Yazawa, Y. Nakagawa, Y. Sasaki, S. Yajima, Effects of alkyl parabens on plant pathogenic fungi. Bioorganic Med. Chem. Lett. 25 (2015) 1774–1777.

[13] A. Asfaram, M. Ghaedi, S. Agarwal, I. Tyagi, V. Kumar Gupta, Removal of basic dye Auramine-O by ZnS: Cu nanoparticles loaded on activated carbon, optimization of parameters using response surface methodology with central composite design. RSC. 5 (2015) 18438–18450.

[14] M. Kiani, S. Bagheri, N. Karachi, E. Alipanahpour Dil, Adsorption of purpurin dye from industrial wastewater using Mn-doped Fe_2O_4 nanoparticles loaded on activated carbon. J. Desal. Water. Treat. 60 (2019) 1-8.

[15] Y. Liu, C. Cui, C. Luo, L. Zhang, Y. Guo, S. Yan, Synthesis of manganese dioxide/iron oxide/graphene oxide magnetic nanocomposites for hexavalent chromium removal. RSC. Adv. 4 (2014) 55162–55172.

[16] S. H. Ahmadi, P. Davar, A. Manbohi, Adsorptive Removal of Reactive Orange 122 from Aqueous Solutions by Ionic Liquid Coated Fe_3O_4 Magnetic Nanoparticles as an Efficient Adsorbent. Iran. J. Chem. Chem. Eng. 35 (2016) 63-73.

[17] W. P. Utomo, E. Santoso, G. Yuhaneka, A.I. Triantini, M.R. Fatqi, M.F. Hudadan, N. Nurfitria, Studi Adsorpsi zat warna Naphthpl Yellow S pada limbah cair Menggunakan aktif dari ampas tebu, Journal. Kimia. (Journal of chemistry). 13 (2019) 104-116.

[18] R. Gaur, P. Jeevanandam, PbS micro-nanostructures with controlled

morphologies by a novel thermal decomposition approach, J. Nanopart. Res. 18 (2016) 80.

[19] K. Suresh Babu, C. Vijayan, R. Devanathan, Strong quantum confinement effects in polymer- based PbS nanostructures prepared by ion-exchange method, Mater. Lett. 58 (2004) 1223- 1226.

[20] J. Liu, H. Yu, Z. Wu, W. Wang, J. Peng, Y. Cao, Size-tunable near-infrared PbS nanoparticles synthesized from lead carboxylate and sulfur with oleylamine as stabilizer, Nanotechnology. 19 (2008) 345602.

[21] G. Long, B. Barman, S. Delikanli, Y. Tsung Tsai, P. Zhang, A. Petrou, H. Zeng, Carrier-dopant exchange interactions in Mn-doped PbS colloidal quantum dots, Appl. Phys. Lett. 101 (2012) 062410.

[22] D. R. Smith, W. J. Padilla, D. C. Vier, S.C. Nemat-Nasser, S. Schultz, Composite medium with simultaneously negative permeability and permittivity, Phys. Rev. Lett. 84 (2000) 4184–4187.

[23] H. Mahmoudi Chenari, B. Ramezanpour, H. Kangarlou, Metamaterial Mn-doped PbS nanoparticles: Synthesis, size-strain linebroadening analysis and Kramers-Kronig study. Ceramics International. 6 (2017) 109.

[24] H. S. Ghazi Mokri, N. Modirshahla, M.A. Behnajady, B. Vahid, Adsorption of C.I. Acid Red 97 dye from aqueous solution onto walnut shell: kinetics, thermodynamics parameters, isotherms. Int. J. Environ. Sci. Technol. 12 (2015) 1401–1408.

[25] Y. Zhao, J. Zou, W. Shi, In situ synthesis and characterization of PbS nano crystallites in the modified hyperbranched polyester by gamma-ray irradiation, Mater. Sci. Eng. 121 (2005) 20-24.

[26] F. Gode, O. Baglayan, E. Guneri, P-Type nano structure PbS Thin films prepared by the silar method. Chalcogenide Letters. 12 (2015) 519-528.

[27] T. S. Shyju, S. Anandhi, R. Sivakumar, R. Gopalakrishnan, Studies on Lead Sulfide (PbS) Semiconducting Thin Films Deposited from Nanoparticles and Its NLO Application. Int. J. NanoScience. 13 (2014) 1450001- 1450012.

[28] M. Ghaedi, B. Sadeghian, A. A. Pebdani, R. Sahraei, A. Daneshfar, C. Duran, Kinetics, thermodynamics and equilibrium evaluation of direct yellow 12 removal by adsorption onto silver nanoparticles loaded activated carbon, Chem. Eng. J. 187 (2012) 133–141.

[29] G. H. Haghdoost, Removal of Reactive Red 120 from Aqueous Solutions Using Albizia lebbeck Fruit (Pod) Partical as a Low Cost Adsorbent, J. Phys. Theore. Chem. 15 (3, 4) (2019) 141-148.

[30] R. Manohar, V. S. Shrivastava, Adsorption removal of carcinogenic acid violet19 dye from aqueous solution by polyaniline-Fe_2O_3 magnetic nano-composite. J. Mater. Environ. Sci. 6 (2015) 11-21.

[31] G. Ghodratollah Absalan, A. Bananejad, M. Ghasemi, Removal of Alizarin Red and Purpurin from Aqueous Solutions Using Fe_3O_4 Magnetic Nanoparticles, Anal. Bioanal. Chem. Res. 4 (2017) 65-77.

[32] Y. S. Ho, G. Mc Kay, The Kinetics of Sorption of Divalent Metal ions onto Sphagnum Moss Peat. Water. Res. 34 (2000) 735-742.

[33] S. Hajati, M. Ghaedi, H. Mazaheri, Removal of methylene blue from aqueous solution by walnut carbon:

optimization using response surface methodology, J. Desal. Water. Treat. 57 (2016) 3179-3193.

[34] S. Hajati, M. Ghaedi, B. Barazesh, F. Karimi, R. Sahraei, A. Daneshfar, A. Asghari, Application of high order derivative spectrophotometry to resolve the spectra overlap between BG and MB for the simultaneous determination of them: ruthenium nanoparticle loaded activated carbon as adsorbent, J. Ind. Eng. Chem. 20 (2014) 2421–2427.

[35] I. Langmuir, The adsorption of gases on plane surfaces of glass, mica and platinum. J. American. Chem. Soc. 40 (1918) 1361–1403.

[36] H. M. F. Freundlich, Over the adsorption in solution. J. Phys. Chem. 57 (1906) 385–470.

[37] M. M. Dubinin, The potential theory of adsorption of gases and vapors for adsorbents with energetically non-uniform surface, Chem. Res. 60 (1960) 235–266.

[38] M. M. Dubinin, Modern state of the theory of volume filling of micropore adsorbents during adsorption of gases and steams on carbon adsorbent, Zh. Fiz. Khim. 39 (1965) 1305 –1317.

[39] M. Toor, B. Jin, Adsorption Characteristics, Isotherm, Kinetics, and Diffusion of Modified Natural Bentonite for Removing Diazo Dye. Chem. Eng. J. 187 (2012) 79-88.

[40] Y. S. Ho, Review of Second-order Models for Adsorption Systems, J. Hazar. Mater. 136 (2006) 681-689.

[41] F. Bouaziz, M. Koubaa, F. Kallel, R.E. Ghorbel, S.E. Chaabouni, Adsorptive Removal of Malachite Green from Aqueous Solutions by Almond Gum: Kinetic Study and Equilibrium Isotherms, Int. J. Biolog. Macromolecules. 105 (2017) 56-65.

[42] S. Banerjee, G.C. Sharma, R.K. Gautam, M.C. Chatto padhyaya, S.N. Upadhyay, Y.C. Sharma, Removal of Malachite Green, a Hazardous Dye from Aqueous Solutions Using Avena Sativa Hull as a Potential Adsorbent, J. Molecular Liquids. 213 (2016) 162-172.

[43] G. H. Vatan khah, A. Kohmareh, Enhanced removal of Bismark Brown (BB) dye from aqueous solutions using activated carbon from raw maize tassel: Equilibrium, thermodynamic and kinetics. J. Phys. Theore. Chem. 14(3) (2018) 237-249.

[44] A. Achmad, J. Kassim, T. Kim Suan, Equilibrium, Kinetic and Thermodynamic Studies on the Adsorption of Direct Dye onto a Novel Green Adsorbent Developed from Uncaria Gambir Extract. J. Phys. Sci. 23 (2012) 1-13.